Formation enthalpies by mixing GGA and GGA + *U* calculations

Anubhav Jain, Geoffroy Hautier, Shyue Ping Ong, Charles J. Moore, Christopher C. Fischer,
Kristin A. Persson, and Gerbrand Ceder[*]
Massachusetts Institute of Technology, 77 Massachusetts Avenue 13-5056, Cambridge, Massachusetts 02139, USA

Standard approximations to the density functional theory exchange-correlation functional have been extraordinary successful, but calculating formation enthalpies of reactions involving compounds with both localized and delocalized electronic states remains challenging. In this work we examine the shortcomings of the generalized gradient approximation (GGA) and GGA + *U* in accurately characterizing such difficult reactions. We then outline a methodology that mixes GGA and GGA + *U* total energies (using known binary formation data for calibration) to more accurately predict formation enthalpies. We demonstrate that for a test set of 49 ternary oxides, our methodology can reduce the mean absolute relative error in calculated formation enthalpies from approximately 7.7–21% in GGA + *U* to under 2%. As another example we show that neither GGA nor GGA + *U* alone accurately reproduces the Fe-P-O phase diagram; however, our mixed methodology successfully predicts all known phases as stable by naturally stitching together GGA and GGA + *U* results. As a final example we demonstrate how our technique can be applied to the calculation of the Li-conversion voltage of $LiFeF_3$. Our results indicate that mixing energies of several functionals represents one avenue to improve the accuracy of total energy computations without affecting the cost of calculation.

I. INTRODUCTION

Density functional theory (DFT) is now capable of accurately computing ground state properties for a variety of materials.[1–4] DFT has its foundations in the Hohenberg-Kohn theorem,[5] which states that all ground state properties of a material (including its total energy) are some unknown functional of its charge density. The most commonly used approximate functionals are those developed in the local density approximations (LDA)[6] or generalized gradient approximations (GGA).[7] Both the LDA and GGA introduce a nonphysical electron self-interaction energy,[8–13] and much of the success of these theories is attributable to the cancellation of this self-interaction energy between the different calculations that are combined into a property. However, predicting relative energies of compounds with very different electronic environments is significantly more challenging as this error cancellation cannot be relied upon.

One method to mitigate the self-interaction error is the GGA + *U* method,[14] which selectively adds an energy correction to localized electron states such as *d* or *f* orbitals for which the self-interaction is particularly large. The GGA + *U* method often correctly reproduces the relative energetics, magnetic ground states, and electronic structure for systems in which GGA fails,[8] including redox reaction energies in oxides for which GGA may produce errors of over 1 eV/f.u..[15,16] However, the GGA + *U* method also suffers from several limitations. In particular the transferability of *U* across compounds is limited. For example, Franchini *et al.* used the GGA + *U* methodology to calculate heats of formation for four binary-manganese oxides (using a single *U* for both metallic Mn and the oxides) and found an average relative error of about 4% after fitting the O_2 energy to minimize the total error.[17] While better than a GGA approach,[17] this still represents a significant error (a 4% relative error in Mn_3O_4 is greater than 0.575 eV/f.u., or about 55 kJ/mol). As we will demonstrate in

this paper, the GGA + *U* framework generally fails to produce the correct energy difference between compounds with localized/correlated and delocalized/uncorrelated electronic states, leading to errors in many technologically relevant quantities, such as ternary-oxide phase diagrams or electrochemical reaction energies such as lithium conversion voltages. This lack of a single functional that reliably describes all chemistries hinders the use of DFT as a predictive tool, especially limiting applications such as high-throughput studies that investigate broad chemical spaces.[18]

Given that DFT seems to be evolving towards functionals that are more specialized for particular chemistries or geometries (e.g., surfaces),[11,19,20] approaches to combine energies calculated with different functionals will be needed. We propose in this paper a technique that, rather than using a single theoretical framework, combines GGA and GGA + *U* energies to improve the formation enthalpies of reactions between compounds with different electronic characteristics. Such an approach is especially appealing because each compound may be computed using the framework that best describes the material. The premise of our approach is that GGA is reasonably accurate in calculating energy differences between compounds with delocalized states,[21] but fails when the degree of electronic localization varies greatly between the products and reactants.[15,18] GGA + *U*, on the other hand, performs well when studying reactions between compounds with localized states (e.g., oxide-to-oxide reactions). Our approach adjusts the GGA + *U* energies using known experimental binary formation enthalpies in a way that makes them compatible with GGA energies. Although energy calibrations based on comparison with experimental formation enthalpies have been suggested in the past,[15,22] we believe this is the first framework that attempts to systematically mix GGA and GGA + *U* energies. We present evidence that such a mixed approach more accurately reproduces the relative energies of compounds

with delocalized and localized states than either technique by itself.

Before proceeding, we mention that new functionals beyond GGA or GGA + U may better represent transitions from delocalized to localized electronic states. For example, hybrid methods that mix in a fraction of Hartree-Fock exact-exchange energy represent one possible improvement as the Hartree-Fock method explicitly cancels the self-interaction energy. In particular the HSE06[10,23,24] hybrid functional has been shown to accurately reproduce redox energies without the need to introduce the U framework.[17,25] However, further investigation of the HSE06 is still needed to clarify its accuracy against GGA + U within both insulating and metallic systems. For example, recent evidence indicates that the HSE06 does not accurately reproduce phase stability in some oxide mixtures.[26] Our mixed GGA/GGA + U method is also less computationally expensive than HSE06; in their study of oxides, Chevrier *et al.* reported about 40 times higher computational expense to use the HSE06 functional than GGA + U.[25]

II. COMPUTATIONAL METHODOLOGY

We used the Vienna Ab Initio Simulation Package (VASP)[27,28] for our calculations in conjunction with the GGA functional[29] as parameterized by Perdew, Burke, and Ernzerhof.[30] The core states were modeled with projector-augmented wave pseudopotentials,[31] and the plane-wave energy cutoff was set to 1.3 times the maximum cutoff specified by the pseudopotentials of the elements in the VASP software.[32,33] We used a k-point grid of $(500)/n$ points, where n represents the number of atoms in the unit cell, distributed as uniformly as possible in k-space with a Gamma-Centered grid for hexagonal cells and a Monkhorst-Pack grid[34] for all others. All compounds were initialized with the crystal structure information as reported in the Inorganic Crystal Structure Database (ICSD)[35,36] and structurally optimized in two consecutive runs using the AFLOW software.[37] We set the electronic energy difference required for convergence to 5×10^{-5}eV $\times n$, and the energy difference required for ionic convergence to 10 times that for electronic energy convergence. Data regarding the accuracy of these parameters can be found in a previous paper.[18] For binary oxides we tested multiple magnetic configurations for a single unit cell using an automated algorithm; for ternary oxides, we initialized all calculations ferromagnetically only.

Unless otherwise specified, we used a 1.36-eV energy adjustment to the O_2 molecule to correct for the GGA binding energy and correlation errors as suggested by Wang *et al.*[15]

We used the rotationally invariant approach to GGA + U proposed by Dudarev,[38] in which the total energy can be expressed as

$$E^{\text{GGA}+U} = E^{\text{GGA}} + \frac{U-J}{2} \sum_{\sigma} \left[\left(\sum_m n_{m,m}^{\sigma} \right) - \left(\sum_{m,m'} n_{m,m'}^{\sigma} n_{m',m}^{\sigma} \right) \right]. \quad (1)$$

TABLE I. U values used in this work for all oxide systems. Multiple values for Wang *et al.* indicate fits to different reactions; for details see Ref. 15. We also present in the last column the energy adjustments that are used to adjust GGA + U energies (derived in Sec. III B).

Element	U value used in this work (oxides, eV)	U values fit by Wang *et al.*[15]	Average ΔE_{M} (eV)
V	3.1	3.0, 3.1, 3.3	1.764
Cr	3.5	3.5	2.067
Mn	3.9	3.5, 3.8, 4.0	1.687
Fe	4.0	3.9, 4.1	1.723
Co	3.4	3.3	1.751
Ni	6.0	6.4	2.164
Cu	4.0	4.0	1.156
Mo	3.5	N/A	2.668

In Eq. (1) n represents the occupation matrix of $3d$ orbitals with the subscripts m representing the d-orbital index (angular momentum quantum number) and σ indexing the spin. The onsite Coulomb parameter U and the exchange parameter J are combined into a spherically averaged, single effective interaction parameter, U-J. We will henceforth refer to this effective interaction parameter simply as U. In addition to correcting the orbital energies of the localized d states, the correction term pushes orbital occupancies toward integer occupations for which $n = n^2$ (or equivalently $n = \{0,1\}$). Such a formulation thereby helps avoid errors in standard DFT functionals caused by a continuous derivative of exchange-correlation energy with electron number, which often leads (usually incorrectly) to partially occupied d bands. Further discussion of the GGA + U method and its application can be found in a review by Anisimov *et al.*[8]

We fit U values according to the methodology of Wang *et al.*,[15] averaging the U value over several reactions. Our resulting values are in close agreement with Wang *et al.*'s previous work (Table I).[15]

Our reaction enthalpies are computed at 0 K and 0 atm and neglect zero-point effects. We believe this approximation is acceptable because heat capacity and density differences between solid phases are generally quite small, leading to only small effects of temperature and pressure. One estimate by Lany, for example, suggests that the difference between ΔH^{298K} and ΔH^{0K} is typically less than 0.03 eV/atom.[22]

III. THEORETICAL FRAMEWORK

A. Basis of theory

The essence of our technique to mix GGA and GGA + U results is to decompose general formation reactions as a set of subreactions. The subreactions are chosen such that each reaction is

(a) well represented by GGA alone,

(b) well represented by GGA + U alone, or

(c) a formation reaction of a binary compound with localized states with known (e.g., experimentally tabulated) reaction energy. In our examples this will be the oxidation reaction of a metal.
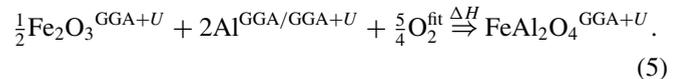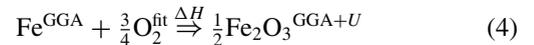
In general we consider reactions involving metals and metal alloys to be well represented by GGA [i.e., category (a)].[39] We also consider main group compounds that do not contain localized d or f states (e.g., Li_2O) to be in this category.[15] The GGA + U category (b) includes reactions between compounds with localized or correlated electronic states.[13,15,40] For the remainder of this paper we focus on the transition-metal oxides as the localized compounds of interest (in Sec. IV C, however, we apply our technique also to fluorides). Finally we use experimental data for reactions (c) involving the formation of localized/correlated binary compounds from the elements. Our motivation for selecting binary-formation enthalpies as the class of reactions (c) is two-fold. First, such reactions bridge the gap between GGA and GGA + U because they include both compounds that we expect to be accurate within GGA (the elements) and compounds that we expect to be accurate within GGA + U (localized/correlated binary oxides). Second, the energies of these binary-formation reactions are generally well-tabulated in the experimental literature, making our adjustments easier to determine from a practical standpoint. Our calculation methodology is schematically shown in Fig. 1.

As an illustrative example of how to decompose reaction energies using the method specified previously, we consider the formation of $FeAl_2O_4$ from FeAl, Al, and O:

$$FeAl + Al + 2O_2 \overset{\Delta H}{\Rightarrow} FeAl_2O_4. \quad (2)$$

The reaction energy of [2] is challenging to calculate because the electronic environment of the product $FeAl_2O_4$ is much more localized than that of the reactants, which implies that one cannot rely on cancellation of self-interaction errors. The conventional way to compute the energy of reaction [2] is to use either GGA or GGA + U for the

entire reaction. However, standard GGA underestimates the formation enthalpy of reaction [2] by 0.930 eV compared to the experimental value of -19.861 eV.[41–43] Meanwhile GGA + U (with $U = 4.0$ applied to Fe d orbitals in FeAl and $FeAl_2O_4$) underestimates the formation enthalpy of reaction [2] by 0.984 eV. We hypothesize that the solution to this problem is to somehow represent FeAl in GGA but $FeAl_2O_4$ in GGA + U according to the outline in Fig. 1. We can accomplish this by splitting reaction [2] into three subreactions, introducing an intermediate binary-oxide formation reaction for Fe_2O_3:

$$FeAl^{GGA} \overset{\Delta H}{\Rightarrow} Fe^{GGA} + Al^{GGA/GGA+U} \quad (3)$$

$$Fe^{GGA} + \tfrac{3}{4}O_2^{fit} \overset{\Delta H}{\Rightarrow} \tfrac{1}{2}Fe_2O_3^{GGA+U} \quad (4)$$

$$\tfrac{1}{2}Fe_2O_3^{GGA+U} + 2Al^{GGA/GGA+U} + \tfrac{5}{4}O_2^{fit} \overset{\Delta H}{\Rightarrow} FeAl_2O_4^{GGA+U}. \quad (5)$$

The sum of these reactions reproduces reaction [2], and each compound is labeled by the framework by which the computation should be performed according to our proposed guidelines. We have labeled metallic Al with both GGA and GGA + U labels because we do not apply a U correction to Al (Table I), thereby making the GGA and GGA + U techniques equivalent. We label O_2 with the label 'fit' because we employ the energy adjustments suggested by Wang *et al.*[15] Finally we note that reaction [5] contains a transition from metallic Al with delocalized states to Al with more localized states in $FeAl_2O_4$. However, the error of transferring electrons from s and p metals is already accounted for in the O_2 correction as determined by Wang *et al.*,[15] and so we expect this reaction to be accurately reproduced using GGA with U applied only to Fe d orbitals.

We can now compute each reaction enthalpy under different computational methodologies and then add the results to predict the overall reaction enthalpy. We expect that reaction [4] will be in error because it mixes GGA and GGA + U calculations without any energy adjustments. Later in this section we will quantify this error and remove it by adding an energy adjustment based on known experimental data.

The enthalpy of reaction [3] is overestimated by 0.126 eV in GGA, and the enthalpy of reaction [5] is underestimated by only 0.012 eV/atom in GGA + U. Therefore, in the case of $FeAl_2O_4$ formation, both GGA and GGA + U are fairly accurate within their realm of application. Assuming the energy of reaction [4] is adjusted to produce no error, the total error in reactions [3]–[5] is only about 0.114 eV, which represents a very substantial improvement over both the GGA methodology (error of 0.930 eV/atom) and the GGA + U methodology (error of 0.984 eV/atom). Removing the error of the binary formation reaction [4] thereby provides the opportunity for substantial improvements over conventional reaction energy predictions.

To remove the error of binary formation reactions, in general we propose that the energy of all GGA + U calculations be adjusted via the equation

$$E_{compound}^{GGA+U \; renorm.} = E_{compound}^{GGA+U} - \sum_M n_M \Delta E_M. \quad (6)$$
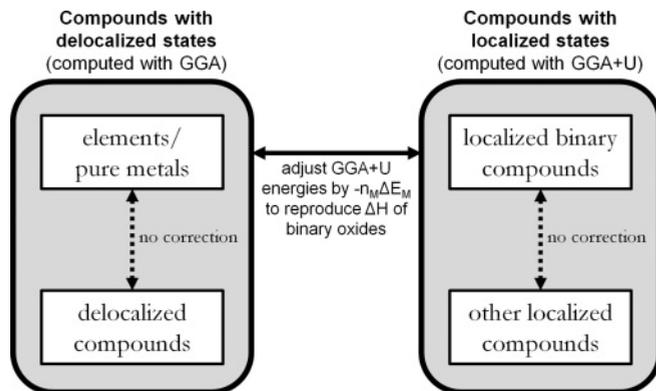

FIG. 1. (Color online) Calculation methodology for mixing GGA and GGA + U calculations. The elements and all delocalized/ uncorrelated compounds are computed with GGA. We compute with GGA + U all localized compounds; in this work, this includes any oxide containing one of the elements listed in Table I. Other types of localized compounds, such as transition metal sulfides or fluorides, might also fall within the realm of GGA + U calculation. The energy adjustment applied to GGA + U can be envisioned as a virtual reaction between the elements and localized binary compounds that is determined using experimental data. This energy adjustment is described in Eq. (6); details are provided in the surrounding text.
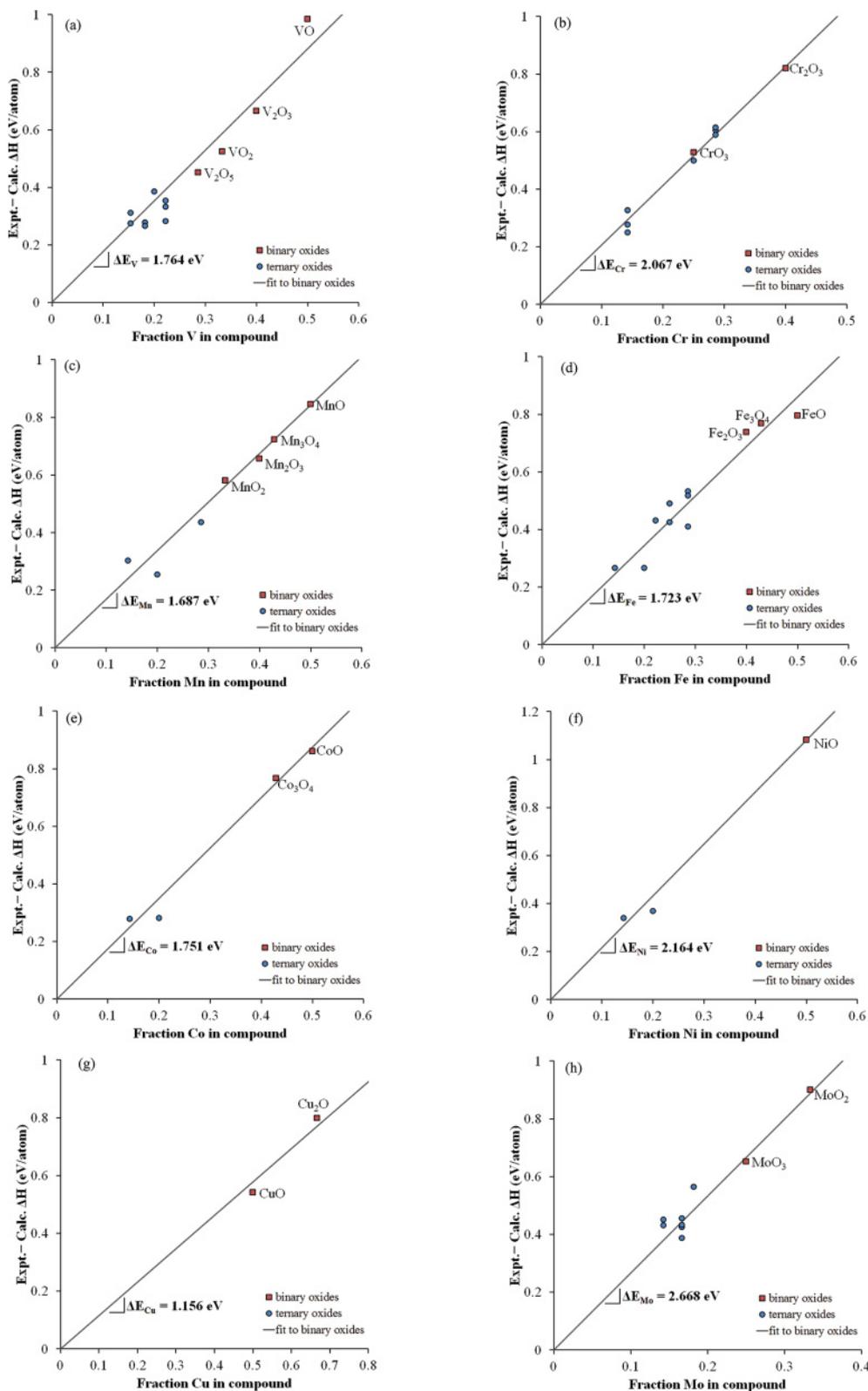
FIG. 2. (Color online) Differences between experimental and calculated and formation enthalpies as a function of metal content for V, Cr, Mn, Fe, Co, Ni, Cu, and Mo. The calculations used GGA for the metals and GGA + U for the binary and ternary oxides. The differences from experiment increase linearly with metal content in the oxides; this difference can be removed simply by adjusting GGA + U energies for the oxides via Eq. (6). The gray line is fitted via least-squares to the binary-oxide data alone (red squares), and its slope represents the magnitude of the adjustment ΔE_M, which is specific to the metal and U value. However, ternary oxides are also well represented by this line, suggesting that the adjustment generalizes beyond the binary oxides.

In Eq. (6) M represents the set of metals which have a U value applied (listed in Table I). The number of M atoms in a compound is represented by n_M, and the error in the binary-oxide formation enthalpy (per metal atom) is represented by ΔE_M. We will fit ΔE_M for various metals M in Sec. III B. Equation (6) subtracts out the error in the binary-formation enthalpies similar to reaction [4], in essence allowing reactions to be broken down into GGA and GGA + U components but connected by a 'virtual' binary formation reaction.

We emphasize that the correction in Eq. (6) is formulated such that it only affects reaction energies that mix GGA and GGA + U calculations. A reaction energy computed purely in GGA + U (such as reaction [5]) will contain the same correction to the reactants and to the product and thereby be completely cancelled. Similarly, a reaction energy computed purely in GGA (such as reaction [3]) will contain no corrections because the proposed framework only adjusts GGA + U energies. The adjustment only affects computations which 'bridge' GGA and GGA + U calculations, such as reaction [4].

B. Transition metal fits

We now attempt to determine the errors ΔE_M for various transition metals so that we may use Eq. (6) to adjust GGA + U energies. One method to find ΔE_M is to pick a single binary-formation reaction for each metal, such as the Fe_2O_3 formation reaction [4] for Fe, and compute the difference between the calculated and experimentally reported enthalpy of reaction. However, to provide a more robust fit and to demonstrate that the error ΔE_M does not depend much on the particular reaction selected, we simultaneously fit ΔE_M using several binary-formation enthalpies for each metal. We focus on binary-oxide reactions because our U values (listed in Table I) are intended for oxides.

For each metal we compute the energies of multiple reactions of the form

$$M^{GGA} + \frac{x}{2}O_2^{fit} \overset{\Delta H}{\Rightarrow} MO_x^{GGA+U}, \qquad (7)$$

for which the reaction enthalpy is listed in the Kubaschewski tables.[41] We note that in Eq. (7) the metal is calculated in standard GGA, whereas the metal oxide is computed in GGA + U. The correction ΔE_M is determined as the average difference between the experimental and computed formation enthalpy for each of these reactions [normalized per metal, as in Eq. (7)].

Figure 2 shows the difference between the uncorrected calculated reaction energies and experimental values. The enthalpy differences in Fig. 2 are normalized per atom and plotted as a fraction of metal content in the compound. In this representation the correction ΔE_M is represented by the slope of the least-squares regression line that passes through the origin. This method of viewing the data helps demonstrate the validity of our decision to add a correction proportional to metal content: the difference between experimental and calculated reaction enthalpies in Fig. 2 clearly depends linearly on metal fraction for the binary oxides as is suggested by Eq. (6). To further demonstrate this trend, we also plot in Fig. 2 the differences in ternary-oxide formation enthalpies from the elements (blue circles). Because the ternary-oxide
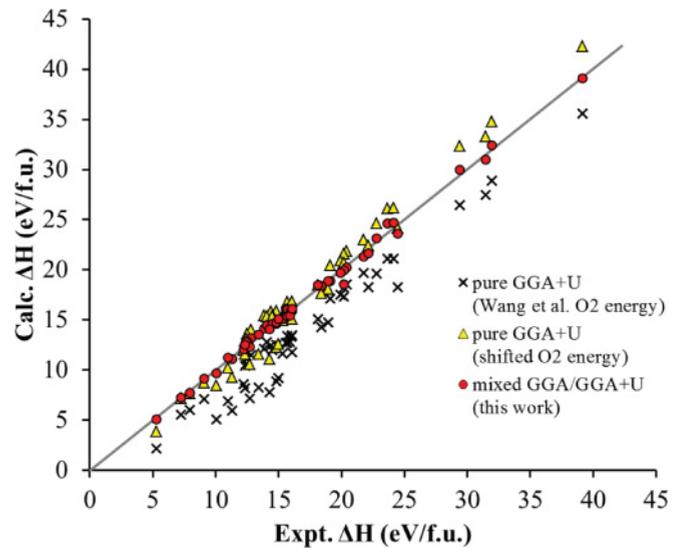

FIG. 3. (Color online) Computed and experimental formation enthalpies of ternary oxides from the elements using (a) GGA + U for all compounds with Wang's O_2 correction, (b) GGA + U with an O_2 correction fitted to minimize the MARE, and (c) the mixed GGA/GGA + U framework proposed in this paper. The mixed GGA/GGA + U framework best reproduces experimental results while retaining an O_2 energy consistent with GGA calculations. The full list of compounds and results can be found in the Appendix.

data falls roughly on the line obtained from the binary oxides, we can be more confident that the adjustments that are fit to binary oxides generalize well to multicomponent oxides. The full ternary-oxide data set is presented in the Appendix, and a full list of our adjusted values is compiled in Table I.

IV. RESULTS

A. Test set of 49 ternary-oxide formation enthalpies

We test the applicability of our mixed GGA/GGA + U energies in reproducing 49 ternary-oxide formation enthalpies from the Kubaschewski tables[41] versus standard GGA + U. We restricted our test set to mixed-metal oxides and avoided polyanion systems (e.g., phosphates, sulfates, borates, etc.) because we believe other systematic errors in GGA may be present for these systems.[18] The compound set includes the ternary oxides from Fig. 2 and adds compounds that contain multiple corrected metals. The full list of compounds we tested along with our computational results is presented in the Appendix. We emphasize that all our energy adjustments were fit only to binary oxides and not to any compound in this test set.

In Fig. 3 we compare formation enthalpies calculated in three different ways. The first method, represented by black 'x' data markers, uses standard GGA + U to compute both metal and compound energies along with Wang *et al.*'s O_2 energy fit.[15] Figure 3 demonstrates that the GGA + U calculations poorly represent the experimental data, showing a mean absolute error (MAE) of 464 meV/atom [a mean absolute relative error (MARE) of over 21%]. We believe

this reflects the failure of $GGA + U$ to properly capture the energetics of delocalized metallic states. To improve the standard $GGA + U$ results, we follow the work of Franchini *et al.*,[17] fitting an alternate correction to the O_2 energy. The yellow triangles in Fig. 3 represent pure $GGA + U$ formation enthalpies in which the O_2 energy has been set to a value that minimizes the MARE over the data set. We find this O_2 energy to be 0.166 eV/atom higher than the energy fit by Wang *et al.*[15] This refitted O_2 energy removes a large portion of the pure $GGA + U$ error, moving the MAE down to 172 meV/atom (MARE down to approximately 7.7%). However, although producing more accurate results, refitting the O_2 energy creates the problem of conflicting O_2 energies: one O_2 energy is accurate for nontransition metal-oxide formation enthalpies[15] and another is accurate for transition metal-oxide formation enthalpies. This problem can be avoided and even more accurate results can be obtained by using the GGA and $GGA + U$ mixing scheme proposed in this paper with Wang *et al.*'s original O_2 energy[15] (red circles). In this method we have used GGA to compute the metals, $GGA + U$ to compute the ternary oxides, and shifted the $GGA + U$ energies using Eq. (6) and the adjustments from Sec. III B. The MAE using our shifting method is approximately 45 meV/atom (MARE under 2%), representing a significant improvement over all standard $GGA + U$ results. This supports our hypothesis that most of the error in reaction energies occurs when electronic states on transition metals change their localization character, and this error may be corrected by applying an energy adjustment proportional to the transition metal content.

B. Application to ternary Fe-P-O phase diagram

Thus far we have emphasized formation enthalpies from the elements, but our methodology also generalizes to arbitrary reactions. To demonstrate how our framework seamlessly mixes GGA and $GGA + U$ calculations, we compute the phase diagram for the Fe-P-O system using methods described previously[44] and using source crystal structures from the ICSD.[35,36] Such a phase diagram is challenging to predict from first principles because its construction requires comparing energies between compounds that are largely delocalized in their electronic states (e.g., elemental Fe) largely covalent (e.g., FeP) and largely localized/correlated (e.g., Fe_2O_3). We consider a phase diagram successful if it reproduces the compositions from the ICSD (which are known to exist experimentally) as stable on the phase diagram.

We present three phase diagrams: one computed using pure GGA for all compounds, a second computed using pure $GGA + U$ for all compounds, and a third using our mixed $GGA/GGA + U$ framework. Wang *et al.*'s O_2 fit is used in all cases; we note that using our refit $GGA + U$ O_2 energy from Sec. IV A does not change the phase diagram. We display graphically in Fig. 4 our computation strategy for the mixed-phase diagram: we use $GGA + U$ for all compounds containing both Fe and O (e.g., Fe_2O_3, $FePO_4$) and GGA for all other compounds.

The pure GGA phase diagram we compute is shown in Fig. 5(a). As the GGA formalism is generally considered

quite successful for compounds that do not contain localized orbitals, the Fe-P compositional line correctly reproduces the phases FeP_4, FeP_2, FeP, Fe_2P, and Fe_3P as stable. However, the Fe-O composition line hints at a failure of GGA for the oxides; no compound near the composition FeO is found to be stable. This failure is even more apparent when looking at ternary Fe-P-O compounds; several important compounds, such as $Fe_2P_2O_7$ and $Fe_3(PO_4)_2$, are absent. Thus a pure GGA phase diagram is not able to accurately treat all systems in the Fe-P-O compositional range. We attribute this failure to the well-studied problem of GGA producing poor energies for compounds containing localized *d*-bands such as transition metal oxides.

The standard $GGA + U$ phase diagram is shown in Fig. 5(b). As we expect, the $GGA + U$ formalism corrects the self-interaction error in materials containing localized orbitals so that the Fe-O binary and Fe-P-O ternary compounds are more correctly modeled. The Fe-O binary system, for example, shows a stable phase $Fe_{14}O_{15}$ near the FeO composition. The standard $GGA + U$ formalism also correctly reproduces $Fe_2P_2O_7$ and $Fe_3(PO_4)_2$ as stable phases. However, $GGA + U$ fails along the Fe-P line where self-interaction is not as high as in the oxides; several important Fe-P phases, including FeP and FeP_2, are not found to be stable within the $GGA + U$ framework. Therefore, while $GGA + U$ correctly identifies the stable oxides, it fails in the regions of the phase diagram containing equilibria between compounds with more delocalized states.

The phase diagram produced using the mixed GGA and $GGA + U$ technique outlined in this paper, Fig. 5(c), successfully reproduces the Fe-P-O phases in all areas of the phase diagram, in essence acting like $GGA + U$ in the regions with high self-interaction and like GGA in regions with low-self interaction. All the phases found individually by either GGA alone or by $GGA + U$ alone are simultaneously present on the mixed $GGA/GGA + U$ phase diagram, showing how our framework in essence naturally stitches together the successful results from GGA and $GGA + U$. The energy adjustments we propose thereby lead to a more accurate representation of the entire Fe-P-O phase diagram under a unified framework.
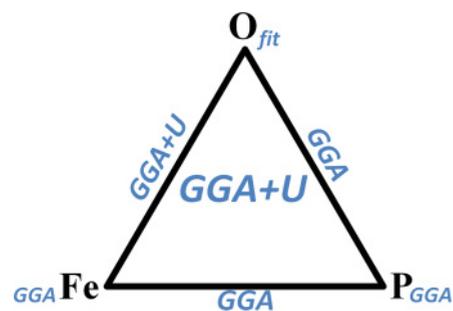

FIG. 4. (Color online) Strategy for generating the Fe-P-O phase diagram using a mixture of GGA and $GGA + U$ calculations. Regions of the phase diagram containing both Fe and O are computed with $GGA + U$, whereas the remaining regions are computed with GGA. This strategy follows the more general guidelines outlined in Fig. 1. The O_2 energy is taken from Wang *et al.*'s fit.[15]
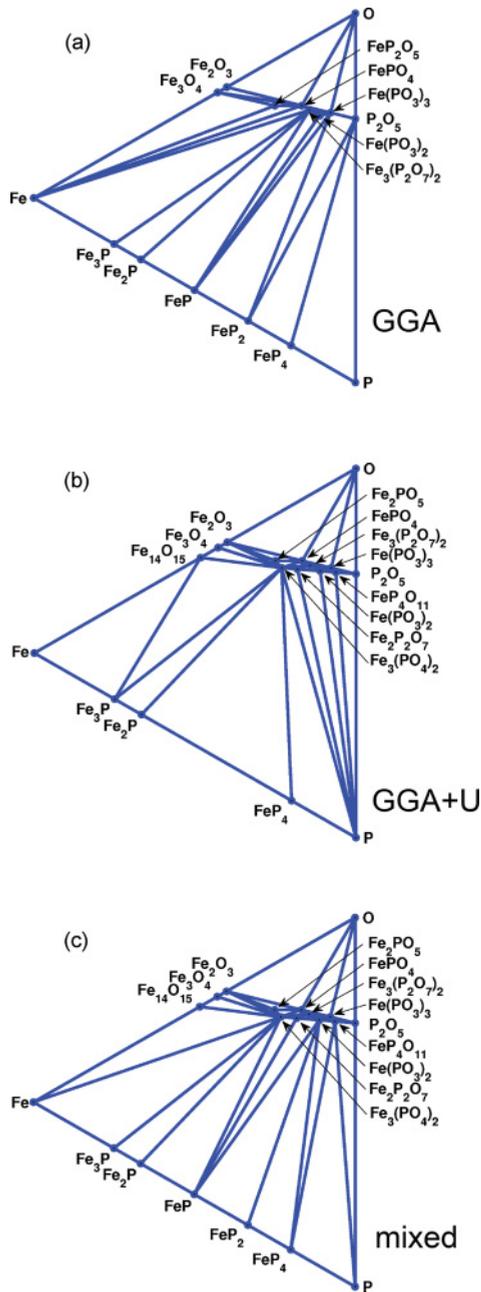
FIG. 5. (Color online) Computed 0 K, 0 atm phase diagram of the Fe-P-O system within the (a) GGA methodology, (b) GGA $+ U$ methodology, and (c) mixed GGA/GGA $+ U$ technique of the current work. The GGA phase diagram fails to reproduce known phases in the Fe-O and Fe-P-O composition ranges, whereas the GGA $+ U$ methodology fails along the Fe-P line. Only the mixed GGA/GGA $+ U$ phase diagram of the current work successfully reproduces known phases in all composition areas.
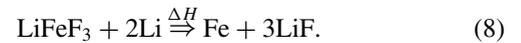
C. Application to Li ion electrode-conversion voltages

One potential technological application of our work is the study of voltages in Li ion battery-conversion electrodes. Conversion electrodes differ from typical intercalation electrodes used in commercial Li ion batteries in that the electrode undergoes a structural transformation during the incorporation of Li. Conversion electrodes offer the potential for higher

energy densities but pose other problems, such as reduced battery cyclability and lower Coulombic efficiency; a review of this topic can be found elsewhere.[45]

The GGA error in predicting Li intercalation voltages in oxides has been previously discussed by Zhou *et al.*[40] and is attributed to the electron transfer from the metallic state in Li metal to a localized transition metal d state in the oxide. It has now been amply demonstrated that such reaction energies can be well predicted by using GGA $+ U$ on the transition-metal oxides. However, in conversion electrodes *both* Li and the transition metal undergo transformations between their metallic states and oxidized states.

For example, one such electrode is LiFeF$_3$, which is believed[46,47] to incorporate Li via the reaction

$$\text{LiFeF}_3 + 2\text{Li} \overset{\Delta H}{\Rightarrow} \text{Fe} + 3\text{LiF}. \qquad (8)$$

The electrochemical voltage of reaction [8], which is approximately equal to $\Delta \text{H}/2$,[48] was calculated by Doe *et al.* to be 2.91 V using GGA.[47] The measured potential, averaged between charge and discharge, is close to 2.5 V (although difficulties exist to ascertain it more accurately than about 0.1 V attributable to polarization in experiments).[46] Doe *et al.* attributed the GGA error to the difficulty in simultaneously modeling the delocalized states of Fe and the localized states of LiFeF$_3$ and subsequently fit the Fe energy using known FeF$_2$ and LiF enthalpies.[47] With the fitted Fe energy, Doe *et al.* arrived at a calculated potential of 2.62 V,[47] in somewhat better agreement with experiments. However, Doe *et al.* only fit corrections to pure GGA energies and never intended to use the Fe correction outside the space of Fe fluorides. Indeed it was unclear whether the GGA error in the reaction was rooted in the Fe energy, the LiFeF$_3$ energy, or some combination.

Here, we show that the same accuracy can be obtained using our methodology that mixes GGA and GGA $+ U$ calculations. Although we are now working in the space of fluorides, we use the U value and element shift determined for binary oxides (compiled in Table I) to determine the voltage of reaction [8] under a mixed GGA/GGA $+ U$ scheme. Our strategy, in accordance with Fig. 1, is to use standard GGA for Fe and LiF and to use GGA $+ U$ adjusted by Eq. (6) for LiFeF$_3$.

We summarize our results in Table II. We calculate a voltage of 2.60 V under our mixed scheme, virtually identical to Doe *et al.*'s fitted results, but without an explicit fit to any fluoride data. For comparison, the pure GGA $+ U$ voltage for reaction [8] is 3.46 V, far from the measured voltage. Therefore, the calculation of conversion-electrode voltages represents another area where the results from multiple functionals may outperform results from a single functional.

V. DISCUSSION

We have outlined a procedure by which energies may be calculated using different theoretical frameworks (GGA and GGA $+ U$) but then adjusted so that relative energies between the frameworks are properly reproduced. This allows one to divide chemical space into regions which are better represented

TABLE II. Experimental and calculated voltages of LiFeF$_3$ decomposition according to reaction [8]. The results of our work reproduce the accuracy of Doe *et al.*'s fitted calculation but without fitting to any Fe fluoride data. The GGA + *U* results are much worse, showing large disagreement with the measured voltage.

Experiment[46]	Doe *et al.* GGA[47]	Doe *et al.* GGA, fitted Fe[47]	GGA/GGA + *U* mixing, this work	GGA + *U*
∼2.5V	2.91V	2.62V	2.60V	3.46V

by either GGA or by GGA + *U* (Fig. 1) but still having the possibility of predicting energies of reactions which cross both spaces. This was demonstrated in Sec. IV A where we accurately predicted ternary-oxide formation enthalpies from the elements, in Sec. IV B where we demonstrated how GGA and GGA + *U* calculations could be stitched together to create a Fe-P-O phase diagram that matched experimental observations, and in Sec. IV C where we successfully reproduced the conversion voltage of an LiFeF$_3$ electrode.

We note that the particular adjustments reported in this work depend on the *U* parameter employed and will need to be refit from the values listed in Table I if different *U* values are used. In addition our adjustments depend on the particular O$_2$ energy used. Although we have reported good results using the energy correction proposed by Wang *et al.*,[15] the adjustments would need to be refit should a different O$_2$ energy be more applicable.

We assume in this work that within a chemical class such as the oxides, a single *U* value for each metal can describe the entire class. However, previous studies have shown that even within a single chemical class (oxides, phosphates, etc.), the optimal *U* values for a metal may vary between compounds or depend on the particular property being investigated.[9,13,49] Our assumption of a single *U* value for each metal, while common in the literature, may thus limit the accuracy of the results obtained with our technique. We note that it is possible to extend our method so that a single metal may have several *U* parameters provided that appropriate experimental data exists. For example, we may choose to apply *U* = 4.0 for Fe *d* orbitals in oxides but *U* = 1.9 for Fe *d* orbitals in sulfides.[18] In this case all Fe compounds with *U* = 4.0 would use an energy-adjustment fit using binary-oxide data, whereas all Fe compounds with *U* = 1.9 would use an energy-adjustment fit using binary-sulfide data only. Alternatively we could attempt to fit different *U* values for Fe^{2+} and Fe^{3+} and calibrate each class using only binary data with the appropriate oxidation state. The number of divisions possible for a single metal is limited by the amount of relevant experimental reaction data available. In essence the schematic concept of Fig. 1 can be extended to more than two functionals and chemical spaces. As long as the compounds in the spaces can be connected through simple reactions for which accurate data can be obtained, the approach described in this paper can be applied. While we used experimental data to connect GGA and GGA + *U* calculations, one could also use more accurate and computationally expensive approaches to obtain the energies of the small set of reactions that connect these spaces.

Despite these limitations we have shown that mixing GGA and GGA + *U* results performs well even in challenging

situations such as reproducing the Fe-P-O phase diagram while adding no additional computational cost over standard GGA + *U* calculations. It is currently unclear whether functionals beyond GGA, such as the hybrid techniques mentioned in Sec. I, would produce more accurate results despite their greater computational expense. The formation enthalpies of binary-transition metal oxides, for example, were found by Chevrier *et al.* to have a fairly large average error of 0.35 eV per O$_2$ using the HSE06 functional.[25] This average error cannot be directly compared with our technique because our adjustments are fit to binary-oxide data. However, it seems likely that HSE06 alone will not produce metal-to-oxide reaction energies that are accurate enough for many applications. This suggests the greater need for techniques to mix results from several functionals, each of which is specialized for a more narrow chemical space.

VI. CONCLUSION

In this work we have demonstrated a procedure by which experimental data can calibrate an adjustment that allows direct comparison between GGA and GGA + *U* energies. We can envision such a framework as dividing formation reactions into subreactions that are accurate in GGA alone, accurate in GGA + *U* alone, or are reactions with tabulated formation enthalpies. We applied this framework to model ternary-oxide formation enthalpies more accurately than a pure GGA + *U* scheme, showing that mean absolute relative errors could be reduced from 7.5–21% to less than 2%. In addition we demonstrated that our methodology could successfully reproduce the ternary-phase diagram of the Fe-P-O system in which either the GGA or GGA + *U* formalisms alone failed to reproduce all known phases in this system. We presented some evidence of applicability of our approach beyond oxides into the fluorides by successfully computing the reaction voltage of the LiFeF$_3$ conversion electrode. Our results indicate that the general approach of mixing results from several specialized functionals present a promising opportunity to improve the accuracy of challenging total energy computations.

APPENDIX

TABLE III. Ternary oxides investigated in this work. Enthalpies of formation are presented for experimental data,[41] GGA + U alone using oxygen corrections from Wang *et al.*[15] and from this work, and mixed GGA/GGA + U with the element corrections proposed in this work.

Formula	expt ΔH (eV/f.u.)	GGA + U ΔH (Wang *et al.* O_2) (eV/f.u.)	GGA + U ΔH (fitted O_2) (eV/f.u.)	GGA/GGA + U ΔH (this work) (eV/f.u.)
V compounds				
BaV_2O_6	23.651	21.109	26.134	24.637
$Ca_3V_2O_8$	39.153	35.587	42.287	39.115
$Ca_2V_2O_7$	31.951	28.889	34.751	32.417
CaV_2O_6	24.136	21.142	26.167	24.670
MgV_2O_6	22.809	19.626	24.651	23.154
$Mg_2V_2O_7$	29.379	26.460	32.323	29.988
Na_3VO_4	19.085	17.092	20.442	18.856
$Na_4V_2O_7$	31.478	27.438	33.301	30.966
$NaVO_3$	12.350	10.422	12.934	12.186
Cr compounds				
$CaCr_2O_4$	18.963	14.732	18.082	18.860
Cs_2CrO_4	14.814	12.534	15.884	14.598
K_2CrO_4	14.409	12.476	15.826	14.540
$MgCr_2O_4$	18.425	14.310	17.660	18.438
$NaCrO_2$	9.084	7.090	8.765	9.154
Na_2CrO_4	13.829	12.086	15.436	14.150
$ZnCr_2O_4$	16.045	11.753	15.103	15.881
Mn compounds				
$MnAl_2O_4$	21.769	19.661	23.011	21.345
Mn_2TiO_4	18.137	15.094	18.444	18.462
$MnTiO_3$	14.085	12.817	15.330	14.501
Fe compounds				
$Ca_2Fe_2O_5$	22.115	18.241	22.428	21.682
$CaFe_2O_4$	15.334	11.618	14.968	15.059
$FeAl_2O_4$	20.381	18.525	21.875	20.246
Fe_2TiO_4	15.559	12.697	16.047	16.138
$FeTiO_3$	12.827	11.497	14.010	13.218
$LiFeO_2$	7.970	6.012	7.687	7.733
$NaFeO_2$	7.237	5.540	7.215	7.261
$ZnFe_2O_4$	12.220	8.604	11.954	12.045
Co compounds				
$CoAl_2O_4$	20.177	18.233	21.583	19.984
$CoTiO_3$	12.515	11.110	13.623	12.861
Ni compounds				
$NiAl_2O_4$	19.904	17.541	20.891	19.696
$NiTiO_3$	12.459	10.623	13.136	12.778
Cu compounds				
$CuAl_2O_4$	20.177	17.355	20.705	18.511
Mo compounds				
$BaMoO_4$	15.715	13.404	16.754	16.060
$CaMoO_4$	16.023	13.307	16.657	15.963
Cs_2MoO_4	15.698	12.699	16.049	15.355
$MgMoO_4$	14.514	11.979	15.329	14.636
Na_2MoO_4	15.902	12.763	16.113	15.419
$Na_2Mo_2O_7$	24.470	18.296	24.158	23.608
$SrMoO_4$	16.057	13.474	16.824	16.131
Mixed compounds				
$CoCr_2O_4$	14.844	8.878	12.228	14.757
$MnFe_2O_4$	12.736	7.181	10.531	12.306
$FeCr_2O_4$	14.991	9.227	12.577	15.076
$CoFe_2O_4$	11.283	5.943	9.293	11.135
$CuFeO_2$	5.317	2.198	3.873	5.074
$CuFe_2O_4$	10.043	5.098	8.448	9.695
$NiCr_2O_4$	14.258	7.779	11.129	14.062
$CuCr_2O_4$	13.404	8.259	11.609	13.543
$MnMoO_4$	12.350	8.207	11.557	12.548
$FeMoO_4$	10.988	6.888	10.238	11.265

*Corresponding author: gceder@mit.edu

[1] G. Ceder, G. Hautier, A. Jain, and S. P. Ong, MRS Bull. **36**, 185 (2011).

[2] K. Kang, Y. S. Meng, J. Bréger, C. P. Grey, and G. Ceder, Science **311**, 977 (2006).

[3] J. Wang, J. B. Neaton, H. Zheng, V. Nagarajan, S. B. Ogale, B. Liu, D. Viehland, V. Vaithyanathan, D. G. Schlom, U. V. Waghmare, N. A. Spaldin, K. M. Rabe, M. Wuttig, and R. Ramesh, Science **299**, 1719 (2003).

[4] G. K. H. Madsen, J. Am. Chem. Soc. **128**, 12140 (2006).

[5] P. Hohenberg, Phys. Rev. **136**, B864 (1964).

[6] W. Kohn and L. J. Sham, Phys. Rev. **140**, 1133 (1965).

[7] D. C. Langreth and J. P. Perdew, Phys. Rev. B **21**, 5469 (1980).

[8] V. I. Anisimov, F. Aryasetiawan, and A. I. Lichtenstein, J. Phys. Condens. Matter **9**, 767 (1997).

[9] A. Rohrbach, J. Hafner, and G. Kresse, J. Phys. Condens. Matter **15**, 979 (2003).

[10] J. Heyd, J. E. Peralta, G. E. Scuseria, and R. L. Martin, J. Chem. Phys. **123**, 174101 (2005).

[11] D. Rappoport, N. R. M. Crawford, F. Furche, and K. Burke, *Computational Inorganic and Bioinorganic Chemistry*, edited by E. I. Solomon, R. B. King, and R. A. Scott (Wiley, Chichester. Hoboken: Wiley, John & Sons, Inc., 2009).

[12] G. I. Csonka, J. P. Perdew, A. Ruzsinszky, P. H. T. Philipsen, S. Lebègue, J. Paier, O. A. Vydrov, and J. G. Ángyán, Phys. Rev. B **79**, 155107 (2009).

[13] F. Zhou, M. Cococcioni, C. A. Marianetti, D. Morgan, and G. Ceder, Phys. Rev. B **70**, 235121 (2004).

[14] V. I. Anisimov, J. Zaanen, and O. K. Andersen, Phys. Rev. B **44**, 943 (1991).

[15] L. Wang, T. Maxisch, and G. Ceder, Phys. Rev. B **73**, 195107 (2006).

[16] F. Zhou, M. Cococcioni, C. A. Marianetti, D. Morgan, and G. Ceder, Phys. Rev. B **70**, 235121 (2004).

[17] C. Franchini, R. Podloucky, J. Paier, M. Marsman, and G. Kresse, Phys. Rev. B **75**, 195128 (2007).

[18] A. Jain, G. Hautier, C. J. Moore, S. P. Ong, C. C. Fischer, T. Mueller, K. A. Persson, and G. Ceder, Comput. Mater. Sci. **50**, 2295 (2011).

[19] A. E. Mattsson, R. Armiento, J. Paier, G. Kresse, J. M. Wills, and T. R. Mattsson, J. Chem. Phys. **128**, 084714 (2008).

[20] M. M. Quintal, A. Karton, M. A. Iron, A. D. Boese, and J. M. L. Martin, J. Phys. Chem. A **110**, 709 (2006).

[21] S. Curtarolo, D. Morgan, and G. Ceder, Calphad **29**, 163 (2005).

[22] S. Lany, Phys. Rev. B **78**, 245207 (2008).

[23] J. Heyd, G. E. Scuseria, and M. Ernzerhof, J. Chem. Phys. **118**, 8207 (2003).

[24] J. Heyd, G. E. Scuseria, and M. Ernzerhof, J. Chem. Phys. **124**, 219906 (2006).

[25] V. L. Chevrier, S. P. Ong, R. Armiento, M. K. Y. Chan, and G. Ceder, Phys. Rev. B **82**, 075122 (2010).

[26] S. P. Ong, V. L. Chevrier, and G. Ceder, Phys. Rev. B **83**, 075112 (2011).

[27] G. Kresse and J. Furthmüller, Phys. Rev. B **54**, 11169 (1996).

[28] G. Kresse and J. Furthmüller, Comput. Mater. Sci. **6**, 15 (1996).

[29] D. C. Langreth and M. J. Mehl, Phys. Rev. B **28**, 1809 (1983).

[30] J. P. Perdew, K. Burke, and M. Ernzerhof, Phys. Rev. Lett. **77**, 3865 (1996).

[31] P. E. Blöchl, Phys. Rev. B **50**, 953 (1994).

[32] G. Kresse and D. Joubert, Phys. Rev. B **59**, 1758 (1999).

[33] G. Kresse, M. Marsman, and J. Furthmüller, VASP the guide, 2010 [http://cms.mpi.univie.ac.at/vasp/vasp/vasp.html].

[34] H. J. Monkhorst and J. D. Pack, Phys. Rev. B **13**, 5188 (1976).

[35] G. Bergerhoff, R. Hundt, R. Sievers, and I. D. Brown, Journal of Chemical Information and Computer Sciences **23**, 66 (1983).

[36] Fiz Karlsruhe, *The Inorganic Crystal Structure Database* [http://icsd.fiz-karlsruhe.de/icsd/]

[37] W. Setyawan and S. Curtarolo, Comput. Mater. Sci. **49**, 299 (2010).

[38] S. L. Dudarev, G. A. Botton, S. Y. Savrasov, C. J. Humphreys, and A. P. Sutton, Phys. Rev. B **57**, 1505 (1998).

[39] S. Curtarolo, D. Morgan, K. Persson, J. Rodgers, and G. Ceder, Phys. Rev. Lett. **91**, 135503 (2003).

[40] F. Zhou, M. Cococcioni, K. Kang, and G. Ceder, Electrochem. Commun. **6**, 1144 (2004).

[41] O. Kubaschewski, C. B. Alcock, and P. J. Spencer, *Materials Thermochemistry*, 6th ed. (Pergamom Press, Oxford, 1993).

[42] K. Rzyman, Calphad **24**, 309 (2000).

[43] O. Kubaschewski and W. A. Dench, Acta Metall. **3**, 258 (1955).

[44] S. P. Ong, L. Wang, B. Kang, and G. Ceder, Chem. Mater. **20**, 1798 (2008).

[45] J. Cabana, L. Monconduit, D. Larcher, and M. R. Palacín, Adv. Mater. **22**, E170 (2010).

[46] F. Badway, F. Cosandey, N. Pereira, and G. G. Amatucci, J. Electrochem. Soc. **150**, A1318 (2003).

[47] R. E. Doe, K. A. Persson, Y. S. Meng, and G. Ceder, Chem. Mater. **20**, 5274 (2008).

[48] M. K. Aydinol, A. F. Kohan, G. Ceder, K. Cho, and J. Joannopoulos, Phys. Rev. B **56**, 1354 (1997).

[49] C. Loschen, J. Carrasco, K. Neyman, and F. Illas, Phys. Rev. B **75**, 035115 (2007).